

P2LHAP:Wearable sensor-based human activity recognition, segmentation and forecast through Patch-to-Label Seq2Seq Transformer

Shuangjian Li, Tao Zhu, *Member, IEEE*, Mingxing Nie, Huansheng Ning, *Senior Member, IEEE*, Zhenyu Liu and Liming Chen *Senior Member, IEEE*

Abstract—Traditional deep learning methods struggle to simultaneously segment, recognize, and forecast human activities from sensor data. This limits their usefulness in many fields such as healthcare and assisted living, where real-time understanding of ongoing and upcoming activities is crucial. This paper introduces P2LHAP, a novel Patch-to-Label Seq2Seq framework that tackles all three tasks in a efficient single-task model. P2LHAP divides sensor data streams into a sequence of "patches", served as input tokens, and outputs a sequence of patch-level activity labels including the predicted future activities. A unique smoothing technique based on surrounding patch labels, is proposed to identify activity boundaries accurately. Additionally, P2LHAP learns patch-level representation by sensor signal channel-independent Transformer encoders and decoders. All channels share embedding and Transformer weights across all sequences. Evaluated on three public datasets, P2LHAP significantly outperforms the state-of-the-art in all three tasks, demonstrating its effectiveness and potential for real-world applications.

Index Terms—sensor-based human activity recognition, activity segmentation, activity forecast, deep learning, Patch-to-Label Seq2Seq framework.

I. INTRODUCTION

THE intersection of deep learning and wearable sensor technology for real-time human activity recognition has emerged as a prominent research focus in recent years. This area holds significant promise for applications in medical health, assisted living, smart homes, and other domains. In various practical scenarios, there is a need for perceptual techniques to delineate activity boundaries, identify activity categories, and predict forthcoming activities from the continuous stream of sensor data. As a result, the field of human activity perception encompasses three pivotal tasks: human activity segmentation (HAS) [1], activity recognition (HAR) [2], and activity forecast (HAF) [5]. While extensive research [3], [4] has addressed each of these tasks individually, limited

This work was supported in part by the National Natural Science Foundation of China (62006110), the Natural Science Foundation of Hunan Province (2024JJ7428, 2023JJ30518) and the Scientific research project of Hunan Provincial Department of Education (22C0229) . (Corresponding author: Tao Zhu.)

Shuangjian Li, Tao Zhu, Mingxing Nie and Zhenyu Liu are with the School of Computer Science, University of South China, 421001 China (e-mail: sjli@stu.usc.edu.cn, tzhu@usc.edu.cn, niemx@usc.edu.cn, lzy@usc.edu.cn). Liming Chen was with School of Computer Science and Technology, Dalian University of Technology, China. Huansheng Ning was Department of Computer & Communication Engineering, University of Science and Technology Beijing, 100083 China (email: l.chen@ulster.ac.uk, ninghuansheng@ustb.edu.cn).

attention has been devoted to simultaneously addressing all three tasks in a cohesive framework.

Several approaches exist for concurrently achieving activity segmentation, recognition, and forecast, as illustrated in Fig. 1. The first approach, shown in Fig. 1(a), employs three independent single-task learning models in parallel. These models output the category of the current activity, the boundary of the current activity, and the category of the next activity. However, this method has drawbacks, including disparate data annotation requirements for different models, the need for additional policies to ensure compatibility among model outputs, and a lack of information sharing between models, leading to inefficient use of computing resources.

A second approach involves multi-task learning in Fig. 1(b), recent advancements in multi-task Human Activity Recognition learning frameworks [7], [8], [21] leverage the interdependences among tasks to facilitate data sharing and encoder learning, enabling the extraction of common data representations. Subsequently, multiple lightweight single-task models are employed. While this approach often enhances multitasking effectiveness, it introduces increased model complexity compared to single-task models. Managing this complexity may necessitate additional computational resources and careful architectural design. Simultaneously, it is crucial to ensure consistency in the model output representation across various tasks. Our objective is to standardize the output representation for improved task-specific adaptability. Furthermore, these multitask models can be more sensitive to hyperparameter choices, demanding meticulous tuning to achieve optimal performance across all tasks.

Different from the first two methods, as shown in Fig. 1(c), this paper proposes a novel Patch-to-Label Seq2Seq framework that tackles all the three human activity perception tasks in a single-task model, named P2LHAP. P2LHAP adopts the encoder-decoder framework, the input is a patch sequence of sensor data, and the output is a sequence of patch-level activity label, where a patch is a short segment of sensor data points. With patch-level labels, it can simply Merge adjacent identical labels to determine the category of the active boundary. In addition, using the encoder-decoder architecture of seq2seq, it can easily output future activity token sequences, making it simple to predict activity label. The architecture handling capability of variable-length sensor activity sequences is excellent, and it exhibits high adaptability to sequences of indefinite length, comprehensively considering

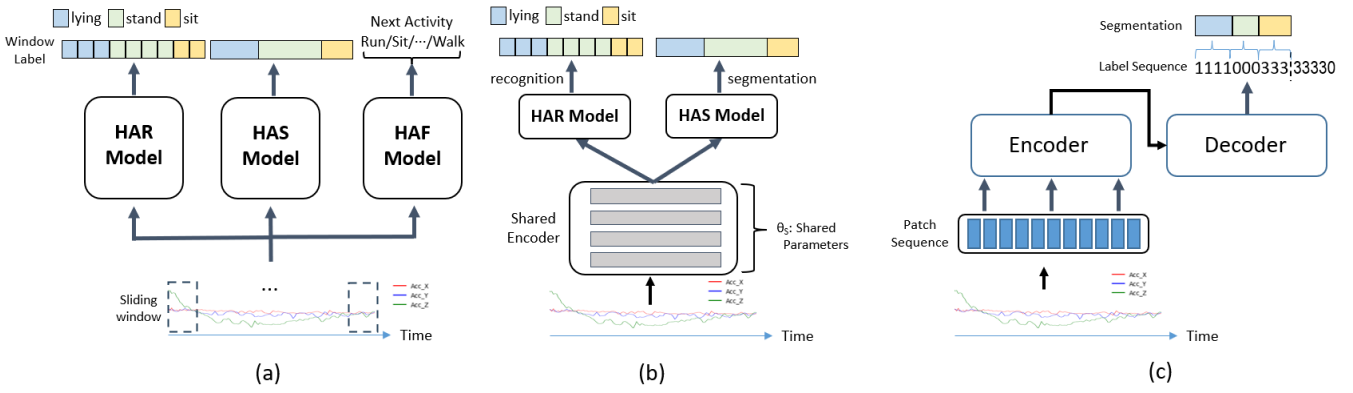


Fig. 1. There are different architectures for multitasking approaches as follows: (a) The data is partitioned using sliding windows, followed by separate training of the respective models. These trained models are subsequently utilized for recognition, segmentation, and forecast. (b) Multi-task methods learn models for multiple tasks through a shared encoder and generate separate results for each task. (c) We propose a multi-task P2L Seq2Seq model specifically designed to generate patch-level active label sequences.

all information within the input sensor signal sequence and effectively retaining the contextual information of the sensor data stream.

Using patches offers several advantages over individual data points and sliding windows. Compared to using single data points [8], [14], using patches can reduce the impact of noise, allowing feature extraction within local intervals [33]. Most existing activity recognition research uses one or more fixed-length sliding Windows to segment the data stream, assuming each window contains a complete activity [7]. However, because activities have varying durations, it is very difficult to set an appropriate window length. If it is too small, the window does not contain enough information; if it is too large, a window contains activities of multiple different categories, both of which will reduce the recognition accuracy [34]. The patching strategy can circumvent this problem well, because we assume that an activity can contain any number of patches, and encoder-decoder architectures such as Transformer are good at handling variable-length sequences, making it feasible to identify activities of arbitrary length.

We introduce a channel-independent Transformer as the encoder-decoder of P2LHAP. Although Transformers have achieved great results in the fields of NLP [9] and CV [36], recent research shows that classic Transformers do not work well on multi-variable long sequence time series prediction problems [35]. This may be because multi-variable features will interfere with the extraction of long-term sequence features [33]. Human activity perception based on wearable devices is essentially a long-sequence multi-variable time series analysis problem. Sensor data includes signals from accelerometers, gyroscopes, magnetometers, etc. Inspired by [33], instead of using the classic Transformer architecture, we introduce a channel-independent Transformer architecture as the encoder-decoder of P2LHAP, each patch only contains data from a single wearable sensor channel information, each sensor signal sequence within the dataset undergoes processing independently within the Transformer model, allowing for the learning of diverse attention patterns tailored to each

sequence. In contrast to the conventional architecture where all sequences are subject to the same attention mechanism, this individualized approach prevents potential interference caused by disparate behaviors within multi-channel sensor data. Moreover, by adopting a channel-independent strategy, the adverse impact of noise prevalent in certain sensor signal sequences can be mitigated as it no longer gets projected onto other sequences within the embedding space.

We utilize the original sensor data sequence along with the patch features obtained from the encoder to compute the representation of individual patches using the attention network to predict activity labels for each patch. Simultaneously, due to the variable size of the patch, the ultimate active label sequence may suffer from over-segmentation. To counter this issue, we devised a smoothing algorithm for the final Patch-level activity label sequence, aimed at mitigating the over-segmentation phenomenon. This algorithm considers the number of activity categories surrounding the patch to adjust the current patch-level activity label. It then establishes activity boundaries based on the label range, thereby mitigating boundary ambiguity in the activity signal to a significant extent.

The main contributions of this paper can be summarized as follows:

- We propose a novel Patch-to-Label Seq2Seq framework that tackles all the three human activity perception tasks in a single-task model, named P2LHAP. To the best of our knowledge, our work constitutes the pioneering effort in unifying activity segmentation, recognition, and forecast within a single framework.
- We employ patches to address the challenge of insufficient information from large sliding windows or individual data points, and our method, utilizing a seq2seq encoder-decoder architecture, readily generates future activity token sequences, making it straightforward to forecast activity labels.
- Each patch of our approach only contains data from a single wearable sensor channel information, each sensor signal sequence within the dataset undergoes processing

independently within the Transformer model, allowing for the learning of diverse attention patterns tailored to each sequence.

- Designed a smoothing method to analyze the number distribution of category labels surrounding each active label. This information is used to update the current active label, effectively reducing the occurrence of over-segmentation errors and providing smoother predictions within the same activity category.
- The proposed P2LHAP method has been evaluated through experiments conducted on three widely used benchmark datasets for activity recognition, segmentation and forecast. The experimental results demonstrate that our approach surpasses existing methods in terms of performance.

II. RELATED WORKS

This section provides a comprehensive review of the progress made in related research on multi-task activity recognition, segmentation, and forecast utilizing sensor signals.

A. Sensor-based activity recognition and segmentation tasks

Sensor-based human activity recognition (HAR) research primarily relies on inertial measurement unit (IMU) sensors found in wearable devices such as smart watches, smart insoles, and sports straps. Due to the limited information contained in a single sample, the common approach for sensor-based activity recognition involves utilizing fixed-size sliding windows, which has shown impressive results [10]. [11], [45] employed a fixed sliding window for sensor data segmentation, followed by a ConvLSTM network to achieve commendable recognition rates. [46] designed an activity recognition model incorporating an attention mechanism and experimentally determined the optimal window size. [50] proposed an adaptive sliding window method and a transition model of body activity to improve classification accuracy. The proposed method adaptively adjusts the window size according to the signal information, but its disadvantage is that the window size can only be expanded dynamically. If the window size can also be reduced to capture short activity signals, the expected performance will be better. Recent studies have employed diverse techniques. [47] distinguished static and dynamic activities using statistical techniques, then classified specific activities with random forests (RF) and CNNs. In [48], NAS was used to investigate effective deep learning (DL) architectures for smartphone inference. [49] introduced a lightweight CNN-BiGRU model, leveraging inertial sensor data from smartwatches and smartphones, achieving satisfactory results. However, the inherent uncertainty in activity duration, these methods will lead to multi-class window problems, where multiple activities may coexist within a window, introducing noise and negatively impacting model recognition performance.

Another effective method for sensor-based activity recognition is dense label prediction [6]. Inspired by the image semantic segmentation task, [?], [?], [14], [15] apply FCN (fully convolutional network) and U-net to sensor-based activity

recognition to predict dense labels, achieving good recognition effects. [16] further proposes Conditional-UNet for coherent human activity recognition with multiple dense labels, explicitly modeling the conditional dependencies between these labels. Current advancements in activity segmentation and recognition, such as [1], [8], leverage dense labeling methods. However, these methods rely solely on individual sensor samples as neural network inputs, and will obtain different representations depending on the task. Our proposed approach employing a patch block, situated between the scales of a large sliding window and a single sample point, for data segmentation. We then utilize a Seq2Seq architecture to unify activity segmentation and recognition tasks, obtaining a unified activity label sequence representation to perform different tasks while mitigating the challenges associated with multi-class windows and over segmentation.

B. forecast of activities using wearable sensors

Sensor-based human activity recognition systems have gained popularity with the widespread use of wearable devices in daily life. However, there is a notable lack of research focusing on sensor-based activity forecast. Recent studies have introduced attention models to predict multivariate motion signals from IMU sensors, thereby preserving pattern and feature information across multiple channels. Predictive models for these time series data can be utilized for human activity forecast by generating and classifying future activity signals. In [17], a combination of a neural network and Fourier transform was employed to convert the sensor activity data into an image format for predicting future signals. In [18] introduced the SynSigGAN model, which utilizes bidirectional grid long short-term memory as the generator network of the GAN model, and a convolutional neural network as the discriminator network to generate future signals. Furthermore, recent work [19] proposes a Transformer-based GAN that can successfully generate real synthetic time series data sequences of arbitrary length, similar to real data sequences. Both the generator and discriminator networks of the GAN model are built using a pure Transformer encoder architecture, which outperforms traditional GAN structures based on RNN or CNN models. Despite these advancements, existing methods predominantly rely on training models to forecast and emulate future sensor activity signals, subsequently employing classification algorithms to derive activity categories from the forecasted signal sequences. Any inaccuracies in the forecasted sensor signals inevitably impact the final classification outcome. In contrast, our proposed P2LHAP architecture bypasses this intermediate step by directly forecasting future activity category token sequences, thereby enhancing forecast accuracy. An additional study [33] presented the PatchTST time series forecast model, which is based on channel independence and patching, and demonstrated promising results. Although progress has been made in multivariate sensor time series data forecast, research on multi-category forecast of human activities based on multi-sensor signal channels remains limited.

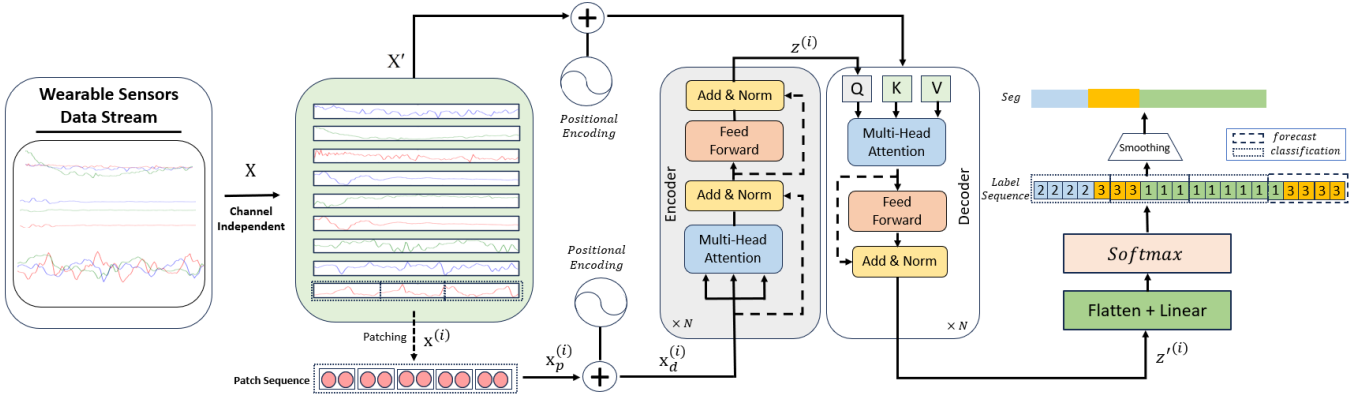


Fig. 2. Overview of the Proposed P2LHAP framework

C. Sensor-based multi-task learning framework

Sensor-based multi-task activity recognition presents a significant challenge in the field. [20] employs recurrent neural networks to segment and identify activities and cycles using inertial sensor data. [21] proposes an efficient multi-task learning framework that utilizes commercial smart insoles. This framework addresses three health management-related problems by converting smart insole sensor data into recursive graphs and employing an improved MobileNetV2 as the backbone network. Experimental results demonstrate that this multi-task learning framework outperforms single-task models in tasks such as activity classification, speed estimation, and weight estimation. [22] introduces a multi-task model based on LSTM for predicting each activity and estimating activity intensity using wearable sensor signals. [8] combines the segmentation and classification tasks by passing the sensor signal through the MS-TCN module to predict sample-level labels and activity boundaries. This joint segmentation and classification approach calculates sample-level loss and boundary consistency loss to achieve improved performance. [7] proposes a novel multi-task framework called MTHARS, which leverages the dynamic characteristics of activity length to segment activities of varying durations through multi-scale window splicing. This approach effectively combines activity segmentation and recognition, leading to improved performance in both tasks. However, prior studies employed distinct backbone networks for various tasks or failed to achieve unified task representations, our proposed architecture integrates these tasks within a single model for simultaneous learning and representation. By doing so, we obtain a unified label sequence representation.

III. METHOD

In this section, we introduce our proposed method, which is a multi-task model for human activity recognition utilizing the Patch-to-Label Seq2Seq approach. Fig. 2 provides an overview of the model's architecture. This model enables activity recognition, segmentation, and forecast tasks on continuous sensor data streams collected from wearable devices. Our

approach consists of three primary components: 1) Patch-to-Label Seq2Seq framework, 2) Patching and channel independent Transformer architecture, and 3) Activity classification, segmentation, and forecasting module.

A. Patch-to-Label Seq2Seq framework

The Patch-to-Label Seq2Seq framework we propose is shown in Fig. 2. We define the M -dimensional input wearable sensor sequence as $\mathbf{X}_{1:L} = [\mathbf{x}_1, \dots, \mathbf{x}_L]$, $\mathbf{x}_t \in \mathbb{R}^{1 \times M}$, where \mathbf{x}_t represents the sensor signals collected at timestamp t . The activity label for each sample is denoted as $y_{1:L} = [y_1, \dots, y_L]$, $y_t \in \mathbb{R}^C$, where C represents the number of activity categories, t is the time step, L is the length of the wearable sensor sequence, and the length of the patch block is defined as P . In this study, we do not employ a fixed-length sliding window to segment the sensor data. The number of patches is denoted as L/P . Our approach utilizes a Transformer encoder and decoder as the underlying framework. To simultaneously process the sensor patch of each channel in parallel within the Transformer backbone, it is crucial to duplicate the Transformer weights multiple times and employ the patching operator to create a sensor sequence sample of a size $B \times M \times L$. The patch-level sequence extends to $M \times P \times N$. Reshaping the dimension sequence into a 3D tensor of size $(B \cdot M) \times P \times N$, the batch of samples serves as the input for the encoder. The purpose of the encoder is to map multiple sequences of single-channel sensor data patches into a latent representation. Following this, the decoder is used to derive the representation of the activity sequence, denoted as $\mathbf{Z}'^{(i)}$. The ultimate output signifies the active label result obtained through the classification head, the active label sequence and the forecast of future activity label sequence of length T_{pre} , denoted as $\hat{y}_{pre} = \{\hat{y}_1, \dots, \hat{y}_{L+T_{pre}}\}$.

B. Patching and channel independent Transformer architecture

1) Patching and channel independent method: We process each sensor signal channel independently, specifically, we segment the input sensor signal sequence $\mathbf{X}_{1:L}$ into M

channel sensor signal sequences $\mathbf{x}^{(i)}$ based on its dimension M , $\mathbf{x}^{(i)}$ represents the sensor sequence of the i -th channel, $i \in \{1, 2, \dots, M\}$. We normalize each $\mathbf{x}^{(i)}$ before patching and the mean and deviation. Next, we divide $\mathbf{x}^{(i)}$ into overlapping or non-overlapping Patches and the length of the Patch block is P . The overlapping part is its step size, represented by S . By segmentation, a patch-level sensor sequence $\mathbf{x}_p^{(i)} \in \mathbb{R}^{1 \times N}$ is obtained, where $N = \left\lfloor \frac{(L-P)}{S} \right\rfloor + 2$. $\mathbf{x}_p^{(N)}$ is the last patch of the segmented patch sequence, this patch is learned through the previous $N-1$ patches, a sequence representation into the future is obtained, with its initial value filled by repeatedly replicating the last number of the original sequence. Finally, we add the corresponding position coding to $\mathbf{x}_p^{(i)}$ to obtain $\mathbf{x}_d^{(i)}$, and then transmit the time series of each channel to the Transformer backbone respectively.

2) **Encoder:** We use the native Transformer encoder [36] to model the features of patch-level sensor sequences, similar to the method used in [33]. The Encoder module utilizes trainable linear projections to map continuous Patch blocks to a D -dimensional Transformer latent space $\mathbf{W}_p \in \mathbb{R}^{D \times P}$. It incorporates a learnable additive positional encoding $\mathbf{W}_{pos} \in \mathbb{R}^{D \times N}$ to capture the temporal order of the patches, represented by $\mathbf{x}_d^{(i)} = \mathbf{W}_p \mathbf{x}_p^{(i)} + \mathbf{W}_{pos}$, where $\mathbf{x}_d^{(i)} \in \mathbb{R}^{D \times N}$ represents the input fed into the Transformer encoder. For each head $h = 1, \dots, H$ in the multi-head attention, the Patch blocks are transformed into query matrices $\mathbf{Q}_h^{(i)} = (\mathbf{x}_d^{(i)})^T \mathbf{W}_h^Q$, key matrices $\mathbf{K}_h^{(i)} = (\mathbf{x}_d^{(i)})^T \mathbf{W}_h^K$, and value matrices $\mathbf{V}_h^{(i)} = (\mathbf{x}_d^{(i)})^T \mathbf{W}_h^V$, where $\mathbf{W}_h^Q, \mathbf{W}_h^K \in \mathbb{R}^{D \times d_k}, \mathbf{W}_h^V \in \mathbb{R}^{D \times D}$. Subsequently, the attention outputs are normalized to obtain the final attention output $\mathbf{Q}_h^{(i)} \in \mathbb{R}^{D \times N}$:

$$(\mathbf{Q}_h^{(i)})^T = \text{Attention}(\mathbf{Q}_h^{(i)}, \mathbf{K}_h^{(i)}, \mathbf{V}_h^{(i)}) \quad (1)$$

$$\text{Attention}(\mathbf{Q}, \mathbf{K}, \mathbf{V}) = \text{softmax}\left(\frac{\mathbf{Q}\mathbf{K}^T}{\sqrt{d_k}}\right)\mathbf{V} \quad (2)$$

The multi-head attention module also includes a BatchNorm layer and a feed-forward network with residual connections.

3) **Decoder:** The Decoder module combines the representation $\mathbf{Z}^{(i)} = \{\mathbf{z}_1, \dots, \mathbf{z}_p\}$, derived from the encoder output, with the corresponding Patch-level wearable sensor data $\mathbf{X}' = \{\mathbf{x}_1', \dots, \mathbf{x}_p'\}$ to generate the activity label sequence using a key-query-value attention mechanism. By multiplying the weight matrices \mathbf{W}_k and \mathbf{W}_v with the Patch-level wearable sensor data, we obtain representations of the key and value, denoted as $\mathbf{K} = \mathbf{W}_k \mathbf{X}'$ and $\mathbf{V} = \mathbf{W}_v \mathbf{X}'$, respectively. At the same time, the query vector \mathbf{Q} is obtained by multiplying the feature representation $\mathbf{z}^{(i)}$ from the encoder with the weight matrix \mathbf{W}_q , expressed as $\mathbf{Q} = \mathbf{W}_q \mathbf{Z}^{(i)}$. Subsequently, the inner product of \mathbf{Q} and \mathbf{K} is passed through a temperature softmax layer to obtain attention scores, which are then used to weigh the summation of the value vector \mathbf{V} , resulting in the representation of $\mathbf{z}'^{(i)}$:

$$\mathbf{z}'^{(i)} = \text{softmax}(\mathbf{Q}^T \mathbf{K} / \sigma) \mathbf{V} = f_\theta(\mathbf{X}', \mathbf{Z}^{(i)}) \quad (3)$$

Here σ is the temperature parameter, and $f_\theta(\cdot)$ represents the attention mechanism network.

C. Activity classification

we employ a Flatten layer with a linear head and a Softmax layer to generate the final human activity label sequence \hat{y} . The representation of \hat{y} is summarized as follows:

$$\text{softmax}(x) = \frac{e^{x_i}}{\sum_{j=1}^n e^{x_j}} \quad (4)$$

$$\hat{y} = \text{argmax}_i(\text{softmax}(\text{Linear}(\mathbf{z}')) \quad (5)$$

During the training phase, we utilize patch-level label predictions and true labels to construct a patch-level classification loss, aiming to effectively optimize the model parameters. This loss is defined as follows:

$$L_{cls} = l_p(\hat{y}, y) \quad (6)$$

Among them, \hat{y} and y represent the patch-level predicted label and the real label, respectively. Given the imbalance of human activity classes under unconstrained conditions, we employ the Softmax CrossEntropy loss function $l_p(\cdot)$ and take into account the number of effective samples for classification. The calculation formula is as follows:

$$l_p(\hat{y}, y) = -\frac{1}{L} \sum_{l=1}^L \sum_{c=1}^C y \log(\hat{y}) \quad (7)$$

Where L signifies the length of input sequence, and C represents the activity class number of dataset. In sensor-based HAR tasks, we leverage this loss function and take into account the number of effective samples to amplify the weight assigned to minority classes. This approach aims to yield fairer and more robust results for each individual class.

D. Activity segmentation and smoothing strategy

Given that the classification loss treats each patch independently, it may result in unwarranted over-segmentation errors. To achieve smoother transitions between patches and minimize over-segmentation errors, we employ the truncated mean square error as our chosen smoothing loss function. The formulation of the smoothing loss is as follows:

$$L_{seg} = L_{T-MSE} = \frac{1}{T_c C} \sum_{t,c} \tilde{\Delta}_{t,c}^2 \quad (8)$$

$$\tilde{\Delta}_{t,c}^2 = \begin{cases} \Delta_{t,c}^2, & \Delta_{t,c} \leq \tau \\ \tau, & \text{otherwise} \end{cases} \quad (9)$$

$$\Delta_{t,c} = |\log \tilde{y}_{t,c} - \log \tilde{y}_{t-1,c}| \quad (10)$$

C represents the activity category, T_c denotes the number of samples belonging to the c -th category, and $\tilde{y}_{t,c}$ signifies the probability of the activity category c being represented by the patch at time t and τ is the smoothing threshold ($\tau = 2$).

For the activity label sequence \hat{y} output by the model, in order to reduce the impact of over-segmentation on subsequent activity merging, we set each activity label as the center, set a smoothing window with a size of `smooth_size`, and set the starting position to the Half of the activity label sequence within the window. Within the window, we count and sort

the activities of each category, and select the activity category with the most surrounding distribution as the current activity label according to the sorting result. After updating the activity label sequence, the performance of activity recognition and segmentation. Finally, it is enhanced by linking Patches of the same activity class to determine the start and end position of each activity in the data flow. We set the boundary set of each activity $B = \{(s_i, e_i)\}_{i=1}^N$, where s_i represents the start subscript of the i -th activity, e_i represents the end subscript of the i -th activity, and N is the number of activities in the activity label sequence. The activity set corresponding to each boundary is represented by $\hat{a} = \{a_i\}_{i=1}^N$, where a_i is the activity corresponding to the i -th boundary. The Process of Algorithm is described in the Algorithm 1.

E. Activity forecasting

Within the activity forecast module, the continuous input Patch blocks retain one Patch block at the end. This involves filling P repeated values of the last $\mathbf{x}_i \in \mathbb{R}$ value at the end of the original sequence. The resulting sequence of generated Patches, $\mathbf{x}_p^{(i)}$, is then represented as $\mathbf{z}'^{(i)} \in \mathbb{R}^{D \times N}$ through the Transformer backbone. By utilizing a linear layer and a fully connected layer with Softmax as the activation function, we obtain the predicted activity sequence, $\hat{y}_{pre} = \hat{y}_{L+1}, \dots, \hat{y}_{L+T_p} \in \mathbb{R}^{1 \times T_p}$, using the representation of the last patch. It is important to note that T_p , the length of the future segment, is determined by the number of Patch blocks within the time T_{pre} , specifically $T_p = \frac{T_{pre}}{P}$.

In the training stage, based on the predicted activity label sequence \hat{y}_{pre} and the ground-truth activity sequence y_{gt} , all patch-level prediction losses can be expressed as:

$$L_{pre} = l_p(\hat{y}_{pre}, y_{gt}) \quad (11)$$

Finally, the previously mentioned loss functions from Equations (6), (8), and (11) are incorporated into the equation, resulting in the final loss function:

$$L = L_{cls} + L_{seg} + L_{pre} \quad (12)$$

We have introduced the main structure of P2LHAP. Algorithm 2 summarizes the training process of P2LHAP.

IV. EXPERIMENTS AND RESULTS

In this section, we provide a comprehensive overview of our experiments and utilize cutting-edge research to evaluate our proposed multi-task framework. Firstly, we present the experimental settings, datasets, and evaluation metrics employed in our study. Subsequently, we perform a series of experiments to assess the effectiveness of our method, including qualitative and quantitative overall performance analysis as well as ablation experiments conducted using the Patch strategy.

A. Experimental setup

Our method was implemented using PyTorch and trained on an RTX 3090 GPU. The batch size was set to 64, and we utilized the Adam optimizer with a learning rate of 0.0001.

Algorithm 1 Segmentation Algorithm

Input: Sensor dataset: \mathbf{X}
Output: Activity label sequence segmentation result: \hat{y}
Activity boundaries: $B = \{(s_i, e_i)\}_{i=1}^N$
Activity class: $\hat{a} = \{a_i\}_{i=1}^N$

- 1: $\hat{y} \leftarrow Model(\mathbf{X})$ by Eq.(1), (2), (3), (4) and Eq(5)
- 2: $smooth_size \leftarrow$ smoothing window size
- 3: set a smooth sequence of active label: $smooth_data \leftarrow []$
- 4: $half_size \leftarrow smooth_size // 2$
- 5: **for** $i = 0$ to $len(\hat{y})$ **do**
- 6: start $\leftarrow \max(0, i - half_size)$
- 7: end $\leftarrow \min(len(\hat{y}), i + half_size + 1)$
- 8: new_activity_label $\leftarrow cal_max(sort(\hat{y}[start : end]))$
- 9: add new_activity_label to smooth_data
- 10: **end for**
- 11: $\hat{y} \leftarrow smooth_data$
- 12: current activity type a $\leftarrow \hat{y}[0]$
- 13: initial activity set index j
- 14: activity start and end index s, e $\leftarrow 0$
- 15: **for** $i = 1$ to $len(\hat{y})$ **do**
- 16: **if** $\hat{y}_i \neq a$ **then**
- 17: Add a to \hat{a}_j
- 18: a $\leftarrow \hat{y}_i$
- 19: e $\leftarrow i$
- 20: Add (s, e) to B
- 21: s $\leftarrow e + 1$
- 22: j $\leftarrow j + 1$
- 23: **end if**
- 24: **end for**

The fully connected dropout rate is set at 20% (0.2), head dropout is fixed at 5% (0.05), the default patch length is 10, with a step size of 10. The model employs 8 heads by default, consists of 6 encoder-decoder layers, and undergoes training for 100 epochs.

For classification, segmentation, and forecast tasks, we employed the entire continuous dataset as input and divided it into training, validation, and test sets with a ratio of 0.7, 0.1, and 0.2 respectively. To evaluate the classification and segmentation performance of the model, we compared the forecast output with the real label. In the forecast task, the forecast patch length was set to 8, and performance assessment was based on a comparison between the forecast output patch label and the real label.

The choice of several parameters values for the models is shown in the table I:

1) *Evaluation metrics:* For the evaluation of the obtained Patch-level label sequences, we use the following metrics:

1. Activity classification

Accuracy: Accuracy is the overall measure of correctness across all classes and is calculated as follows:

$$Accuracy = \frac{\sum_{c=1}^C TP_c + \sum_{c=1}^C TN_c}{\sum_{c=1}^C (TP_c + TN_c + FP_c + FN_c)} \quad (13)$$

Weighted F1 score: The weighted F1 score is calculated based on the proportion of Patch samples:

Algorithm 2 The training process of P2LHAP

Input: Training dataset: $\{\mathbf{X}_{train}, y_{train}\}$
Validation dataset: $\{\mathbf{X}_{val}, y_{val}\}$
Test dataset: $\{\mathbf{X}_{test}, y_{test}\}$

Output: Patch-level activity label predictions: \hat{y}

- 1: Initialize training epoch e , optimizer \leftarrow Adam
- 2: **while** $e \leq Epoch_{max}$ and *Convergent* **do**
- 3: Get a mini-batch data \mathbf{X}_{batch} in \mathbf{X}_{train}
- 4: $\hat{y} \leftarrow Model(\mathbf{X}_{batch})$ by Eq.(1), (2), (3), (4) and Eq.(5)
- 5: $y_{gt} \leftarrow y_{train}$
- 6: $\hat{y}_{pre} \leftarrow \hat{y}[-T_p : -1]$
- 7: Calculate L_{cls} with eq.(6), (7)
- 8: Calculate L_{pre} with eq.(11)
- 9: Get \hat{y}_{seg} through algorithm 1
- 10: $\hat{y} \leftarrow \hat{y}_{seg}$
- 11: Calculate $L_{seg}(\hat{y}, y_{gt})$ with eq.(8)
- 12: $e \leftarrow e + 1$
- 13: Update model parameters based on eq.(12)
- 14: *adjust_learning_rate(optimizer, e, args)*
- 15: Calculate \hat{y}_{val} with Eq.(6), (8) and check convergence
- 16: **end while**
- 17: Update \hat{y} from test sequence \mathbf{X}_{test} based on the model

TABLE I
THE CHOICE OF SEVERAL PARAMETERS VALUES FOR THE MODELS

Model Parameters	Parameters Values	Parameter Introduction
seq_len	200/151/512	input sensor sequence length 200(WISDM)/151(Unimib SHAR)/512(PAMAP2)
pred_len	8	prediction label sequence length
fc_dropout	0.2	fully connected dropout
attn_dropout	0.05	attention dropout
head_dropout	0.00	transformer head dropout
patch_len	10	patch length
stride	10	stride
revin	1	RevIN True: 1 False: 0
enc_in	3/3/9	encoder input size(the number of sensor channels) 3(WISDM)/3(Unimib SHAR)/9(PAMAP2)
dec_in	3/3/9	decoder input size(the number of sensor channels) 3(WISDM)/3(Unimib SHAR)/9(PAMAP2)
n_heads	4	number of transformer heads
e_layers	6	number of encoder layers
d_layers	6	number of decoder layers
d_ff	256	dimension of FCN
class_num	6/17/12	number of activities
d_model	256	dimension of transformer model
s_t	2	smoothing threshold
d_k	d_{model}/n_{heads}	dimension of the query/key vectors per attention head
d_v	d_{model}/n_{heads}	dimension of the value vectors per attention head

$$F_w = \sum_{c=1}^C 2 * w_c \frac{prec_c \cdot recall_c}{prec_c + recall_c} \quad (14)$$

Where $prec_c = \frac{TP_c}{TP_c + FP_c}$ and $recall_c = \frac{TP_c}{TP_c + FN_c}$ represent precision and recall, respectively. The weight w_c is calculated as the ratio of n_c to N , where n_c is the number of Patch samples per class, and N is the total number of Patch samples.

2. Activity segmentation

Jaccard Index: The proposed metric assesses the degree of overlap between actual activity segments and predicted activity segments, specifically focusing on the sensitivity towards over-segmentation errors. For the purpose of representation, G_i and

P_i are introduced as respective variables denoting the actual and predicted activity ranges. In this context, the subscript i signifies the i th segment within class C. The calculation of this metric can be determined utilizing the prescribed formula:

$$JI = \frac{1}{C} \sum_{c=1}^C \frac{G_i \cap P_i}{G_i \cup P_i} \quad (15)$$

3. Activity forecast

Mean Square Error(MSE): MSE serves as a prevalent metric to evaluate the performance of forecast models. It computes the average of the squared differences between predicted values and actual values, thereby providing a quantification of the degree of deviation between the predicted and actual values. A lower MSE signifies a more precise alignment between the model's predictions and the actual values, indicating superior performance. The formula for calculating MSE can be represented as follows:

$$MSE = \frac{1}{n} \sum_{i=1}^n (y_i - \hat{y}_i)^2 \quad (16)$$

B. Datasets

To evaluate our proposed method, we adopt three challenging public HAR datasets: WISDM, PAMAP2, UNIMIB SHAR. A brief introduction to the dataset follows.

WISDM Dataset [23]: The dataset was collected from 29 participants using mobile phones equipped with triaxial accelerometers placed in their pants pockets. The data was sampled at a frequency of 20 Hz. Participants engaged in six activities on a daily basis: Walking, Jogging, Upstairs, Downstairs, sitting, Standing. To address missing values in the dataset, the mean of the corresponding column was used for filling them.

PAMAP2 Dataset [24]: The dataset consists of data collected from nine participants who wore IMUs on their chest, hand, and ankle. These IMUs collected information on acceleration, angular velocity, and magnetic sensors. Each participant was instructed to complete 12 mandatory activities such as lying down, standing, going up and down stairs, as well as 6 optional activities like watching TV, driving, and playing ball.

UNIMIB SHAR Dataset [25]: The dataset was collected by researchers at the University of Milan-Bicocca. Thirty volunteers, ranging in age from 18 to 60 years old, were equipped with Bosch BMA220 sensors on their Samsung mobile phones. The phones were placed in both the participants' left and right pockets, resulting in a total of 11,771 activities recorded. The dataset comprises 17 categories of activities, categorized into two coarse-grained groups: 9 activities of daily living (ADL) and 8 falling behaviors.

C. Comparison algorithm

We compare our method with state-of-the-art algorithms for activity recognition, segmentation, and forecast.

- **MPCC-MRCSE [39]:** A multidimensional parallel convolutional connected (MPCC) deep learning network based

on MMS data for HAR is proposed that fully utilizes the advantages of multidimensional convolutional kernels.

- CNN-BiLSTM [40]: Proposed multibranch CNN-BiLSTM network does automatic feature extraction from the raw sensor data with minimal data pre-processing
- MRFC-VAE-Net [37]: A multi-resolution fusion convolutional network is proposed to make up for the shortcoming that confusing activities are difficult to correctly identify, thereby improving the accuracy of identification.
- Multi-ResAtt [41]: Multi-ResAtt integrates a recurrent neural network with attention to extract time-series features and perform activity recognition.
- ConvAttention [26]: A lightweight multi-head model that incorporates an attention mechanism to enhance the representation capability of CNNs for human activity recognition.
- CE-HAR [38]: Provide an alternative called Channel Equalization to reactivate these inhibited channels by performing whitening or decorrelation operation, which compels all channels to contribute more or less to feature representation
- TripleCrossAttention [28]: This method introduces a triple cross-dimensional attention mechanism for sensor-based activity recognition tasks.
- SK [29]: A multi-branch CNN model that utilizes selective kernel mechanisms for HAR. Additionally, it incorporates attention mechanisms for the first time in the HAR domain to select kernels between multiple branches with different receptive fields (RFs).
- MTHARS [7]: A multi-task deep neural network that enhances activity segmentation and recognition by utilizing a multi-scale window splicing method. This approach effectively combines both tasks and improves performance.
- JSR [8]: A multi-task learning framework for joint segmentation and recognition of activities using wearable sensors. It introduces a multi-level temporal convolutional network (MS-TCN) to predict activities at the sample level, overcoming the challenge of multi-class windows. The consistency loss attention mechanism effectively enhances the consistency between activity and boundary predictions.
- TS-DyConv [43]: A temporal-spatial dynamic convolutional network, to recognize human activity. Temporal-spatial dynamic convolution (TS-DyConv) aims to dynamically learn the convolutional kernels weighted with attention generated along the temporal and spatial kernel spaces.
- MarNASNets [44]: A mobile-aware convolutional neural network (CNN) for sensor-based HAR by NAS (MarNASNets), MarNASNets achieve the same accuracy as the existing CNN architectures with fewer parameters and are effective model architectures for on-device and sensor-based HAR.
- PQ-CNN [47]: Simple statistical techniques are used to distinguish static or dynamic activities, and random forests (RF) and convolutional neural networks (CNN) are used to classify specific activities.
- HS-ResNet [42]: A new CNN that uses hierarchical-split

(HS) idea for a large variety of HAR tasks, which is able to enhance multiscale feature representation ability via capturing a wider range of receptive fields of human activities within one feature layer.

D. Comparisons with activity recognition algorithm

In this section, we compare our method with other competing methods that have been evaluated on three publicly available datasets for wearable-based Human Activity Recognition. To conduct a thorough performance analysis, we use non-overlapping patches of size 10 to compare the overall recognition performance.

We compared the recognition performance of our proposed method with other similar algorithms as mentioned earlier. The recognition performance of various competing methods is summarized in Table II. Our method demonstrated improvements in recognition accuracy across three publicly available HAR datasets. Particularly, on the Unimib and PAMAP2 datasets, our method achieved the highest recognition performance, obtaining weighted average F1 scores of 82.04% and 98.92% respectively. Remarkably, our method surpassed the performance of the leading competing method by 3.26% in terms of weighted average F1 score on the Unimib dataset.

In Fig. 3, we present the confusion matrix of our method for activity classification on the PAMAP2 dataset using patch sizes of 200 and 10, respectively. The confusion matrix provides insight into the accuracy of our method for various activity categories. It is evident that, despite the different patch sizes, there is minimal variation in overall accuracy. However, when the patch size is small, over-segmentation occurs, necessitating active segmentation through dividing the patch blocks. This approach enhances the recognition performance for most activity categories.

E. Qualitative segmentation results

To demonstrate our proposed method's segmentation performance, this section presents a visualization of patch-level activity predictions in Fig. 4, with each color representing a different activity category. We compare sequence fragments obtained through model segmentation with selected sequence fragments from the PAMAP2 and WISDM datasets. In practical application scenarios, excessive segmentation can adversely affect prediction accuracy. Nonetheless, as depicted in the figure, our method successfully reduces most over-segmentation errors, leading to more precise and consistent patch-level predicted segments within each active segment.

Table III displays the segmentation performance of our proposed method in comparison to competing algorithms. Our method excels in both segmentation and recognition tasks, consistently outperforming the comparison algorithms. Specifically, our Jaccard Index results on the Pamap2 dataset surpassed those of A&D and JSR by 9.82% and 3.47% respectively, Where (w/o) represents the segmentation Jaccard Index scores obtained without using the smoothing strategy. This justifies our employment of a smoothing algorithm, which effectively mitigates the boundary irregularities resulting from

TABLE II
ACC AND F₁ PERFORMANCE ON THREE DATASETS.

PAMAP2			WISDM			UNIMIB SHAR		
methods	Acc	F1	methods	Acc	F1	methods	Acc	F1
ours	98.71%	98.92%	ours	97.51%	97.52%	ours	81.51%	82.04%
Y Li et al. (2023) [43]	98.04%	-	K. Xia et al. (2020) [27]	92.71%	92.63%	Y. Tang et al. (2022) [28]	76.30%	75.38%
W. Gao et al. (2021) [29]	93.80%	93.38%	S Kobayashi et al. (2023) [44]	90.62%	-	W. Gao et al. (2021) [29]	75.89%	74.63%
SK. Challa et al. (2022) [40]	94.27%	94.25%	Z. N. Khan et al. (2021) [26]	96.85%	97.20%	F. Duan et al. (2023) [7]	76.48%	75.71%
Al-Qaness et al. (2022) [41]	93.19%	92.96%	W. Gao et al. (2021) [29]	97.51%	97.25%	Al-Qaness et al. (2022) [41]	77.29%	76.83%
F. Duan et al. (2023) [7]	94.50%	94.80%	W. Huang et al. (2023) [38]	99.04%	99.18%	W. Huang et al. (2023) [38]	78.65%	78.78%
W. Huang et al. (2023) [38]	92.14%	92.18%	J. Li et al. (2023) [37]	97.11%	<u>98.64%</u>	Y. Tang et al. (2022) [42]	<u>79.02%</u>	<u>79.19%</u>
S. Xia et al. (2022) [8]	94.59%	94.47%	SK. Challa et al. (2022) [40]	96.04%	96.05%			
J. Li et al. (2023) [37]	97.39%	98.12%	MK. Yi et al. (2023) [47]	96.07%	96.14%			
Y. Wang et al. (2023) [39]	-	98.33%						

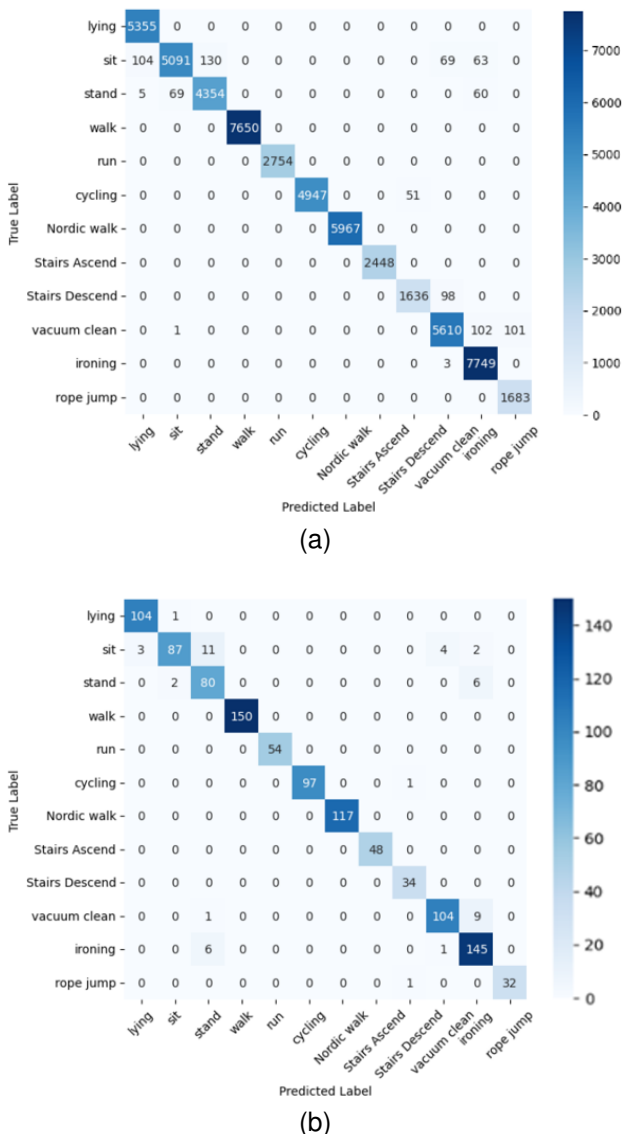


Fig. 3. The confusion matrices on the PAMAP2 dataset for patch sizes of 10 and 200 (a) *Patch_size*=10, (b) *Patch_size*=200

excessive segmentation. The algorithm serves to enhance clarity by refining the boundaries and ensuring a more distinct range for each individual activity.

Sensor-recorded human activity data forms a continuous data stream, encompassing diverse actions like standing, sitting, walking, and transitions such as stand-to-sit and sit-to-lying. These activities are classified into two categories: basic and transition, based on their duration. Basic activities, characterized by longer periods, can be either dynamic (e.g., walking) or static (e.g., sitting), whereas transition activities involve brief actions (seconds), like posture shifts (e.g., sit-to-stand). Despite the prevalence of basic activity research, transition events are frequently overlooked due to their lower frequency and shorter duration compared to basic activities. When considering the short-lived activities that intervene between consecutive basic activities, two distinct scenarios may arise:

- When two consecutive basic activities differ, the activity segments in between are classified as transition activities.
- If adjacent basic activities are identical, the segments in between are designated as the disturbance process of the activity. This occurs due to external influences or human factors disrupting the sensor data, causing irregular fluctuations over time. Consequently, the activities preceding and following the disturbance are considered of the same type.

Given the brief nature of transition activities, our framework efficiently divides the original sensor data into multiple patches, ensuring that the information of these short events can be effectively captured and learned. As demonstrated in Fig. 4(c), the short duration of the Jogging activity does not hinder our framework's ability to accurately segment it, showcasing its effectiveness.

F. Patch forecast analysis

In this section, we assess the performance of the activity forecast module using our model to forecast the duration of activity categories in the next 8 patch blocks. Fig. 5



Fig. 4. Segment visualization results on PAMAP2 and WISDM datasets

TABLE III
RESULTS OF SEGMENTATION METRICS ON PAMAP2 DATASET.

Seg Metric	PAMAP2 DATASET				
	Attn	A&D	JSR	ours(w/o)	Ours
Jaccard Index	0.7908	0.8312	0.8947	0.8445	0.9294

displays the confusion matrix for the future activity forecast in the pamap2 dataset. Fig. 5 (a),(b),(c) present the prediction confusion matrices of Conv2LSTM [30], Seq2Seq-LSTM [31], and Seq2Seq-LSTM-PE-MA [32] predictors for five activity categories in the dataset, while Fig. (d) illustrates the predictions of our proposed model. The confusion matrix results for all campaigns indicate an average accuracy of 96.59%. Additionally, we compare the predicted outputs of future sensor signals with the ground truth signals by evaluating their mean squared error (MSE). To enable the model to predict future sensor signals, we exclude the last classification header and utilize the first half of the input sensor sequence for model input, reserving the second half to match the size of the predicted output data. Table IV presents the performance comparison of our model with five forecasters for sensor sequence signal prediction.

TABLE IV
EVALUATION RESULTS OF THE FORECASTERS.

Metric	Models				
	SynSigGAN	Conv2LSTM	Seq2Seq-LSTM	TTS-GAN	Ours
MSE	0.355	0.302	0.240	0.163	0.126

G. Ablation experiments

In this section, we conduct two ablation experiments to investigate the influence of varying patch block sizes on model performance and the efficacy of patching operations in generating label sequences.

Impact of Patch Size: various sizes and quantities of patches can yield different outcomes. Hence, we employ a scaling approach with multiple patches to analyze their performance. We provide the comprehensive results in Table V. We observed a decrease in accuracy when the Patch size is reduced significantly. This decline can be attributed to the issue of excessive segmentation. However, when the Patch size is set to 10, it consistently exhibits exceptional recognition performance across all three datasets.

The impact of Patching modules: we examined the effects on the results by not patching the sensor data stream, but instead using the Transformer backbone directly. The F1 score obtained on the benchmark dataset is presented in Table VI. It was observed that when the data was not patched during processing, the accuracy of the experimental results deteriorated. Hence, applying data patching enhanced the performance of activity recognition.

The impact of the number of multiple heads and the number of encoder-decoder layers: this study investigates the influence of model components on classification outcomes by varying the number of multi-heads and encoder-decoder layers. Table VII presents the activity recognition accuracy of our proposed framework on the PAMAP2 dataset, showcasing the performance changes with different configurations. The results indicate that an increase in both multi-heads count and model layer depth facilitates better learning of activity sequence representations, leading to enhanced recognition accuracy. The optimal configuration is achieved when the model has 6 layers and 8 multi-heads, achieving the highest accuracy.

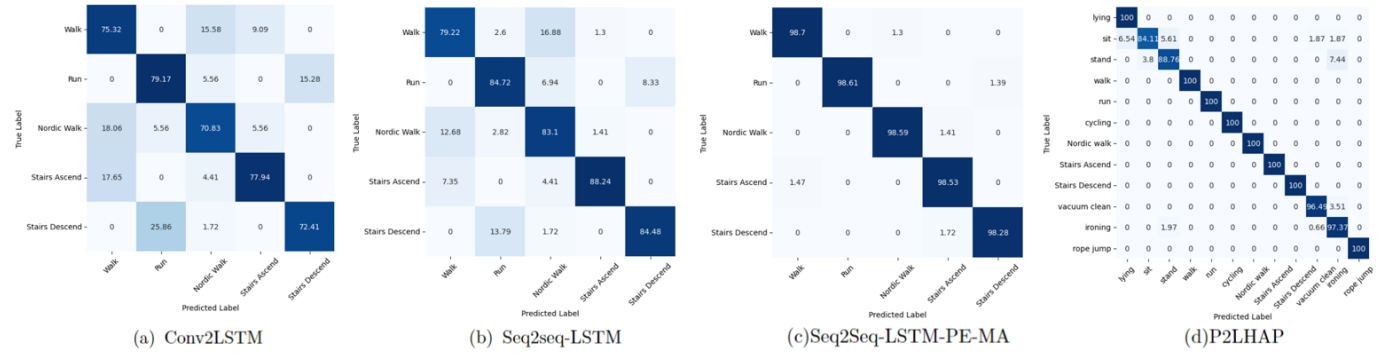


Fig. 5. Confusion matrix of our model and three other models in predicting activity classification results on the PAMAP2 dataset

TABLE V
 F_1 VALUES WITH DIFFERENT PATCH SIZES ON BENCHMARK DATASETS.

Datasets	Patch Size				
	P=1	P=2	P=5	P=10	P=20
WISDM	0.8544	0.9056	0.8819	0.9751	0.9568
PAMAP2	0.9151	0.9406	0.9610	0.9892	0.9667
UNIMIB	0.6719	0.6950	0.7566	0.8204	0.7876

TABLE VI
ACTIVITY CLASSIFICATION F_1 VALUE WITHOUT PATCHING MODULE ON BENCHMARK DATASETS

Model	WISDM	PAMAP2	UNIMIB
only transformer backbone	0.9090	0.8783	0.7533
P2LHAP	0.9752	0.9892	0.8204

H. Further Analysis

To thoroughly assess the practicality of our proposed methodology, we will examine its computational complexity and parameter count, aiming to determine its feasibility for real-time deployment on mobile or embedded devices. The computational analysis was conducted on a Linux platform equipped with an RTX 3090 GPU and an Intel Core i9-13900K. The experiments employed a batch size of 32 for both training and testing, with 3 encoder and decoder layers,

TABLE VII
ACTIVITY RECOGNITION ACCURACY WITH DIFFERENT NUMBERS OF MULTI-HEADS AND DIFFERENT NUMBERS OF ENCODER-DECODER LAYERS ON THE PAMAP2 DATASET

Layer	Multi-heads				
	1	2	4	8	16
1	0.8964	0.9259	0.9372	0.9447	0.9485
2	0.9406	0.9556	0.9560	0.9654	0.9581
3	0.9693	0.9702	0.9633	0.9750	0.9719
6	0.9658	0.9741	0.9793	0.9871	0.9788
8	0.9710	0.9793	0.9790	0.9802	0.9812

and 4 multi-heads. Utilizing the PAMAP2 dataset, we set the input sequence length to 512, patch size to 24, and step size to 12.

The computational complexity comparison, as presented in the table VIII, reveals that our method exhibits superior parameter efficiency and lower inference time compared to the benchmarked techniques.

TABLE VIII
COMPLEXITY COMPARISON OF SEVERAL COMPETING METHODS ON THE PAMAP2 DATASET

Methods	Param	FLOPs	Inference time(s/epoch)
Attn. [13]	1.983M	20.058M	8.22
A&D [12]	1.503M	25.612M	11.88
JSR [8]	2.799M	12.105M	0.78
Ours	1.449M	20.014M	0.08

V. DISCUSSION AND FUTURE WORK

This section delves into the merits and drawbacks of our proposed framework, with a focus on addressing the challenges posed by the inherent uncertainty in natural human activity durations and the complexities of IMU signal analysis for activity segmentation, recognition, and forecast. To tackle these issues, we introduce a novel multi-task deep learning framework that employs the transformer's Patch Sequence to Label Sequence architecture. The transformer network captures inter-patch relationships, enabling it to predict future activity sequences based on past representations. However, our framework's reliance on a closed space assumption in traditional machine learning restricts its ability to handle unknown activities, as the softmax classification layer misclassifies them as known categories. Future work will concentrate on enhancing the architecture to accommodate activity recognition in novel environments, by addressing the issue of unknown activity recognition. Below we will discuss the points planned for improvement in subsequent research:

1) Given that our model employs a Softmax function for classification, its output space is confined, precluding the ability to reject unknown classes, as the predicted probabilities are normalized among all known training classes. Consequently, the model struggles to accurately identify novel activities. To address this limitation, we intend to adopt Deep Open

Classification (DOC) [51] in our future work. Unlike softmax, DOC employs a "1-vs-Rest" layer with N Sigmoid functions for N known classes, which serves as a basis for representing both known and unknown classes. By transferring the learned similarity knowledge from known classes to potential unknowns, we can leverage hierarchical clustering algorithms to cluster rejected instances based on the transferred similarity, thus revealing potential activity classes within the rejected samples.

2) Our model currently adopts a supervised training approach. Future iterations will incorporate self-supervision for retraining, as it eliminates the need for costly labeled datasets in real-world activity recognition scenarios. Self-supervised learning generates training targets autonomously and exploits unlabeled data to learn representations, addressing the challenge of limited labeled data or high annotation costs. This adaptation enhances the model's applicability to practical tasks. Moreover, by facilitating the learning of more universal and general feature representations for unseen activities, self-supervision contributes to improving the model's generalization across diverse activity recognition tasks.

VI. CONCLUSION

In this paper, we propose P2LHAP, an activity-perception model that offers a patch sequence to label sequence model design solution tailored to identify, segment, and forecast human activities through sensor data analysis. Unlike conventional Transformer-based models, P2LHAP partitions the native sensor data stream into multiple patch blocks and utilizes a channel-independent approach to mitigate noise interference among sensor channels. The forecast of forthcoming activity sequences is achieved through reasoning with a Transformer encoder-decoder. To address the issue of over-segmentation, we refine labels based on the nearby distribution of labels close to the active label, thus reducing clutter in the distribution of active labels. Leveraging the P2LHAP framework, we effectively tackle activity segmentation, recognition, and forecast within the realm of activity perception tasks. Our experimental evaluation on three standard datasets demonstrates that our method surpasses existing approaches in classification, segmentation, and forecast tasks.

REFERENCES

- [1] T. Meena and K. Sarawadekar, "Seq2dense u-net: Analyzing sequential inertial sensor data for human activity recognition using dense segmentation model," *IEEE Sensors Journal*, vol. 23, no. 18, pp. 21 544–21 552, 2023.
- [2] L. Chen, R. Hu, M. Wu, and X. Zhou, "Hrgan: A hierarchical multi-modal generative adversarial network model for wearable human activity recognition," *Proceedings of the ACM on Interactive, Mobile, Wearable and Ubiquitous Technologies*, vol. 7, no. 3, pp. 1–27, 2023.
- [3] L. Chen, J. Hoey, C. D. Nugent, D. J. Cook, and Z. Yu, "Sensor-based activity recognition," *IEEE Transactions on Systems, Man, and Cybernetics, Part C (Applications and Reviews)*, vol. 42, no. 6, pp. 790–808, 2012.
- [4] V. Bianchi, M. Bassoli, G. Lombardo, P. Fornacciari, M. Mordonini, and I. De Munari, "Iot wearable sensor and deep learning: An integrated approach for personalized human activity recognition in a smart home environment," *IEEE Internet of Things Journal*, vol. 6, no. 5, pp. 8553–8562, 2019.
- [5] S. Park, H. O. Lee, Y. M. Hwang, S.-K. Ko, and B.-T. Lee, "Enhanced prediction model for human activity using an end-to-end approach," *IEEE Internet of Things Journal*, vol. 10, no. 7, pp. 6031–6041, 2022.
- [6] S. Vandenhende, S. Georgoulis, W. Van Gansbeke, M. Proesmans, D. Dai, and L. Van Gool, "Multi-task learning for dense prediction tasks: A survey," *IEEE Transactions on Pattern Analysis and Machine Intelligence*, vol. 44, no. 7, pp. 3614–3633, 2022.
- [7] F. Duan, T. Zhu, J. Wang, L. Chen, H. Ning, and Y. Wan, "A multi-task deep learning approach for sensor-based human activity recognition and segmentation," *IEEE Transactions on Instrumentation and Measurement*, 2023.
- [8] S. Xia, L. Chu, L. Pei, W. Yu, and R. C. Qiu, "A boundary consistency-aware multitask learning framework for joint activity segmentation and recognition with wearable sensors," *IEEE Transactions on Industrial Informatics*, vol. 19, no. 3, pp. 2984–2996, 2022.
- [9] A. Vaswani, N. Shazeer, N. Parmar, J. Uszkoreit, L. Jones, A. N. Gomez, Ł. Kaiser, and I. Polosukhin, "Attention is all you need," *Advances in neural information processing systems*, vol. 30, 2017.
- [10] K. Chen, D. Zhang, L. Yao, B. Guo, Z. Yu, and Y. Liu, "Deep learning for sensor-based human activity recognition: Overview, challenges, and opportunities," *ACM Computing Surveys (CSUR)*, vol. 54, no. 4, pp. 1–40, 2021.
- [11] F. J. Ordóñez and D. Roggen, "Deep convolutional and lstm recurrent neural networks for multimodal wearable activity recognition," *Sensors*, vol. 16, no. 1, p. 115, 2016.
- [12] A. Abedin, M. Ehsanpour, Q. Shi, H. Rezatofighi, and D. C. Ranasinghe, "Attend and discriminate: Beyond the state-of-the-art for human activity recognition using wearable sensors," *Proceedings of the ACM on Interactive, Mobile, Wearable and Ubiquitous Technologies*, vol. 5, no. 1, pp. 1–22, 2021.
- [13] V. S. Murahari and T. Plötz, "On attention models for human activity recognition," in *Proceedings of the 2018 ACM international symposium on wearable computers*, 2018, pp. 100–103.
- [14] R. Yao, G. Lin, Q. Shi, and D. C. Ranasinghe, "Efficient dense labelling of human activity sequences from wearables using fully convolutional networks," *Pattern Recognition*, vol. 78, pp. 252–266, 2018.
- [15] V. Badrinarayanan, A. Kendall, and R. Cipolla, "Segnet: A deep convolutional encoder-decoder architecture for image segmentation," *IEEE transactions on pattern analysis and machine intelligence*, vol. 39, no. 12, pp. 2481–2495, 2017.
- [16] L. Zhang, W. Zhang, and N. Japkowicz, "Conditional-unet: A condition-aware deep model for coherent human activity recognition from wearables," in *2020 25th International Conference on Pattern Recognition (ICPR)*. IEEE, 2021, pp. 5889–5896.
- [17] T. Kim, J. Park, J. Lee, and J. Park, "Predicting human motion signals using modern deep learning techniques and smartphone sensors," *Sensors*, vol. 21, no. 24, 2021.
- [18] D. Hazra and Y.-C. Byun, "Synsgigan: Generative adversarial networks for synthetic biomedical signal generation," *Biology*, vol. 9, no. 12, 2020.
- [19] X. Li, V. Metsis, H. Wang, and A. H. H. Ngu, "Tts-gan: A transformer-based time-series generative adversarial network," in *Artificial Intelligence in Medicine*, M. Michalowski, S. S. R. Abidi, and S. Abidi, Eds. Cham: Springer International Publishing, 2022, pp. 133–143.
- [20] C. F. Martindale, V. Christlein, P. Klumpp, and B. M. Eskofier, "Wearables-based multi-task gait and activity segmentation using recurrent neural networks," *Neurocomputing*, vol. 432, pp. 250–261, 2021.
- [21] J. Kim, H. Kang, J. Yang, H. Jung, S. Lee, and J. Lee, "Multi-task deep learning for human activity, speed, and body weight estimation using commercial smart insoles," *IEEE Internet of Things Journal*, 2023.
- [22] O. Barut, L. Zhou, and Y. Luo, "Multitask lstm model for human activity recognition and intensity estimation using wearable sensor data," *IEEE Internet of Things Journal*, vol. 7, no. 9, pp. 8760–8768, 2020.
- [23] J. R. Kwapisz, G. M. Weiss, and S. A. Moore, "Activity recognition using cell phone accelerometers," *ACM SigKDD Explorations Newsletter*, vol. 12, no. 2, pp. 74–82, 2011.
- [24] A. Reiss and D. Stricker, "Introducing a new benchmarked dataset for activity monitoring," in *2012 16th international symposium on wearable computers*. IEEE, 2012, pp. 108–109.
- [25] D. Micucci, M. Mobilio, and P. Napoletano, "Unimib shar: A dataset for human activity recognition using acceleration data from smartphones," *Applied Sciences*, vol. 7, no. 10, p. 1101, 2017.
- [26] Z. N. Khan and J. Ahmad, "Attention induced multi-head convolutional neural network for human activity recognition," *Applied soft computing*, vol. 110, p. 107671, 2021.

- [27] K. Xia, J. Huang, and H. Wang, "Lstm-cnn architecture for human activity recognition," *IEEE Access*, vol. 8, pp. 56 855–56 866, 2020.
- [28] Y. Tang, L. Zhang, Q. Teng, F. Min, and A. Song, "Triple cross-domain attention on human activity recognition using wearable sensors," *IEEE Transactions on Emerging Topics in Computational Intelligence*, vol. 6, no. 5, pp. 1167–1176, 2022.
- [29] W. Gao, L. Zhang, W. Huang, F. Min, J. He, and A. Song, "Deep neural networks for sensor-based human activity recognition using selective kernel convolution," *IEEE Transactions on Instrumentation and Measurement*, vol. 70, pp. 1–13, 2021.
- [30] M. Canizo, I. Triguero, A. Conde, and E. Onieva, "Multi-head cnn-rnn for multi-time series anomaly detection: An industrial case study," *Neurocomputing*, vol. 363, pp. 246–260, 2019.
- [31] L. Y. e. a. Wang X., Cai Z., "Long time series deep forecasting with multiscale feature extraction and seq2seq attention mechanism," *Neural Process Lett*, vol. 54, pp. 3443–3466, 2022.
- [32] I. E. Jaramillo, C. Chola, J.-G. Jeong, J.-H. Oh, H. Jung, J.-H. Lee, W. H. Lee, and T.-S. Kim, "Human activity prediction based on forecasted imu activity signals by sequence-to-sequence deep neural networks," *Sensors*, vol. 23, no. 14, p. 6491, 2023.
- [33] Y. Nie, N. H. Nguyen, P. Sinthong, and J. Kalagnanam, "A time series is worth 64 words: Long-term forecasting with transformers," in *International Conference on Learning Representations*, 2023.
- [34] H. Qian, S. J. Pan, and C. Miao, "Weakly-supervised sensor-based activity segmentation and recognition via learning from distributions," *Artificial Intelligence*, vol. 292, p. 103429, 2021.
- [35] A. Zeng, M. Chen, L. Zhang, and Q. Xu, "Are transformers effective for time series forecasting?" in *Proceedings of the AAAI conference on artificial intelligence*, vol. 37, no. 9, 2023, pp. 11 121–11 128.
- [36] A. Dosovitskiy, L. Beyer, A. Kolesnikov, D. Weissenborn, X. Zhai, T. Unterthiner, M. Dehghani, M. Minderer, G. Heigold, S. Gelly, J. Uszkoreit, and N. Houlsby, "An image is worth 16x16 words: Transformers for image recognition at scale," *ICLR*, 2021.
- [37] J. Li, H. Xu, and Y. Wang, "Multiresolution fusion convolutional network for open set human activity recognition," *IEEE Internet of Things Journal*, vol. 10, no. 13, pp. 11 369–11 382, 2023.
- [38] W. Huang, L. Zhang, H. Wu, F. Min, and A. Song, "Channel-equalization-har: A light-weight convolutional neural network for wearable sensor based human activity recognition," *IEEE Transactions on Mobile Computing*, vol. 22, no. 9, pp. 5064–5077, 2023.
- [39] Y. Wang, H. Xu, L. Zheng, G. Zhao, Z. Liu, S. Zhou, M. Wang, and J. Xu, "A multidimensional parallel convolutional connected network based on multisource and multimodal sensor data for human activity recognition," *IEEE Internet of Things Journal*, vol. 10, no. 16, pp. 14 873–14 885, 2023.
- [40] S. K. Challa, A. Kumar, and V. B. Semwal, "A multibranch cnn-bilstm model for human activity recognition using wearable sensor data," *The Visual Computer*, vol. 38, no. 12, pp. 4095–4109, 2022.
- [41] M. A. Al-Qaness, A. Dahou, M. Abd Elaziz, and A. Helmi, "Multi-resatt: Multilevel residual network with attention for human activity recognition using wearable sensors," *IEEE Transactions on Industrial Informatics*, vol. 19, no. 1, pp. 144–152, 2022.
- [42] Y. Tang, L. Zhang, F. Min, and J. He, "Multiscale deep feature learning for human activity recognition using wearable sensors," *IEEE Transactions on Industrial Electronics*, vol. 70, no. 2, pp. 2106–2116, 2022.
- [43] Y. Li, J. Wu, W. Li, A. Fang, and W. Dong, "Temporal-spatial dynamic convolutional neural network for human activity recognition using wearable sensors," *IEEE Transactions on Instrumentation and Measurement*, 2023.
- [44] S. Kobayashi, T. Hasegawa, T. Miyoshi, and M. Koshino, "Marnasnets: Towards cnn model architectures specific to sensor-based human activity recognition," *IEEE Sensors Journal*, 2023.
- [45] J. Yang, M. N. Nguyen, P. P. San, X. Li, and S. Krishnaswamy, "Deep convolutional neural networks on multichannel time series for human activity recognition." in *Ijcai*, vol. 15. Buenos Aires, Argentina, 2015, pp. 3995–4001.
- [46] H. Ma, W. Li, X. Zhang, S. Gao, and S. Lu, "Attnsense: Multi-level attention mechanism for multimodal human activity recognition." in *IJCAI*, 2019, pp. 3109–3115.
- [47] M.-K. Yi, W.-K. Lee, and S. O. Hwang, "A human activity recognition method based on lightweight feature extraction combined with pruned and quantized cnn for wearable device," *IEEE Transactions on Consumer Electronics*, 2023.
- [48] S. Kobayashi, T. Hasegawa, T. Miyoshi, and M. Koshino, "Marnasnets: Toward cnn model architectures specific to sensor-based human activity recognition," *IEEE Sensors Journal*, vol. 23, no. 16, pp. 18 708–18 717, 2023.
- [49] H. A. Imran, Q. Riaz, M. Hussain, H. Tahir, and R. Arshad, "Smart-wearable sensors and cnn-bigru model: A powerful combination for human activity recognition," *IEEE Sensors Journal*, vol. 24, no. 2, pp. 1963–1974, 2024.
- [50] M. H. M. Noor, Z. Salcic, I. Kevin, and K. Wang, "Adaptive sliding window segmentation for physical activity recognition using a single tri-axial accelerometer," *Pervasive and Mobile Computing*, vol. 38, pp. 41–59, 2017.
- [51] L. Shu, H. Xu, and B. Liu, "Doc: Deep open classification of text documents," in *Proceedings of the 2017 Conference on Empirical Methods in Natural Language Processing*, 2017, pp. 2911–2916.